SATSA Mukhapatra - Annual Technical Issue ***30*** *: 2026* ISSN 0971-975X ***Invited Paper***

Digital Modelling of Soil Organic Carbon Using Multiscale Remote Sensing and Ancillary Data

Mani Deshmukh[a], Ayan Das[a,b], Ushasi Dam[a], Kaushik Majumdar[c] and Somsubhra Chakraborty[a,]*

(Received : November 23, 2025; Revised : January 07, 2026; Accepted : January 14, 2026)

ABSTRACT

Understanding how soil organic carbon (SOC) varies across landscapes is essential for sustainable land management. This study used Automatic Machine Learning to generate high-resolution SOC maps for two districts in Gujarat, integrating 1,171 local samples from Anand and Surendranagar with global SOC information from World Soil Information System data and a suite of soil, climate, vegetation, and terrain covariates. All environmental variables were standardized to 30-m resolution for modelling. The Gradient Boosting Machine performed best locally (R^2: 0.49 training, 0.35 testing), while the Stacked Ensemble model showed superior performance globally (R^2: 0.87 training, 0.70 testing). Annual precipitation (the highest-ranked predictor in the local model) and long-term maximum EVI (the most influential variable in the global model) emerged as dominant predictors of SOC across the two modelling scales. The resulting SOC maps can support site-specific soil management, carbon accounting, and climate-resilient land-use planning in data-scarce regions.

Keywords : Soil Organic Carbon, EVI, Automatic Machine Learning

Introduction

Reliable spatial information on soil attributes that regulate landscape functions and ecosystem services is essential for sustainable land management. Since soil organic matter plays a central role in maintaining soil fertility, sustainable agriculture frameworks highlight its careful management (Shibu *et al.*, 2006). Soil organic carbon (SOC) is fundamental to soil functioning: it supports nutrient supply to plants, promotes soil aggregation and structural stability, enhances water-holding capacity, and sustains the soil biotic community (Schoonover and Crim, 2015). Increasing SOC stocks not only improves soil quality and productivity but also contributes to reducing greenhouse gas emissions (Viscarra Rossel *et al.*, 2016). Because soils can sequester carbon at comparatively high rates, they offer substantial potential for mitigating climate change impacts by counterbalancing fossil-fuel-related emissions (Conant *et al.*, 2011; Lal, 2004). Adoption of improved land- and crop-management practices can further increase

[a]Agricultural and Food Engineering Department, Indian Institute of Technology (IIT) Kharagpur, Kharagpur, India
[b]Space Applications Centre, ISRO, Ahmedabad, India
[c]Soil Testing Laboratory, Habra, West Bengal, India
*Corresponding Author Email: somsubhra@agfe.iitkgp.ac.in

yields, particularly in degraded landscapes, thereby supporting food security (Denton *et al.*, 2014). High-resolution SOC maps are therefore valuable both for environmental assessments of carbon sequestration and for agricultural management. For site-specific crop management, digital SOC mapping is especially important (Dobermann and Ping, 2004).

Digital soil mapping (DSM) has become increasingly common for predicting soil properties because it enables efficient spatial estimation using environmental covariates (Lagacherie and McBratney, 2007). DSM is grounded in the CLORPT concept (Jenny, 1941) and its extension, the SCORPAN framework, which relate soil variation to soil (s), climate (c), organisms (o), relief (r), parent material (p), age (a), and spatial position (n) (McBratney *et al.*, 2003). A range of statistical and geostatistical approaches has been applied to model the relationships between these factors and soil attributes. These include regression-kriging (Hengl *et al.*, 2004), decision tree-based models (Henderson *et al.*, 2005), neural networks (Mansuy *et al.*, 2014; Malone *et al.*, 2009), multiple linear regression (Powers and Schlesinger, 2002), and generalized linear models (McKenzie and Ryan, 1999). Accordingly, the aims of the present study were: (i) to build SOC predictive models using both global and local datasets and compare their performance, (ii) to identify the environmental variables most strongly influencing SOC estimates in each modelling framework, and (iii) to produce high-resolution SOC maps for two districts in Gujarat, India.

Materials and Methods

Study Area and Soil Sampling

The study was conducted in Anand and Surendranagar districts of Gujarat, India (Figure 1). Anand lies in alluvial and piedmont plains with mildly calcareous, slightly alkaline, poorly drained soils dominated by Ocrepts and Usterts. Surendranagar comprises shallow medium-black soils derived from Deccan basalts and deep black alluvial soils. Both districts experience high annual temperatures (30.7–31.2°C) and low rainfall (25–34 mm).

Soil samples were collected in March 2018, a period of minimal soil moisture variation. Sampling locations were selected using stratified random sampling based on Sentinel-2 bare soil reflectance and previous-season crop information. At each site, a quincunx (five-point) sampling pattern within a 20–30 m² quadrat was used, with 0–5 cm depth samples composited to ~250 g. GPS coordinates were recorded for each quadrat with an estimated horizontal accuracy of ±3–5 m. SOC was measured using the Walkley and Black (1934) wet oxidation method. Sampling details are provided in Table 1.

Table 1. Specifications of the sites in Gujarat

Place	Area Covered (km^2)	Time of Sampling	No. of soil samples collected
Anand	142.8	March 2018	1081
Surendranagar	431.2	March 2018	90
Total no. of samples			1171

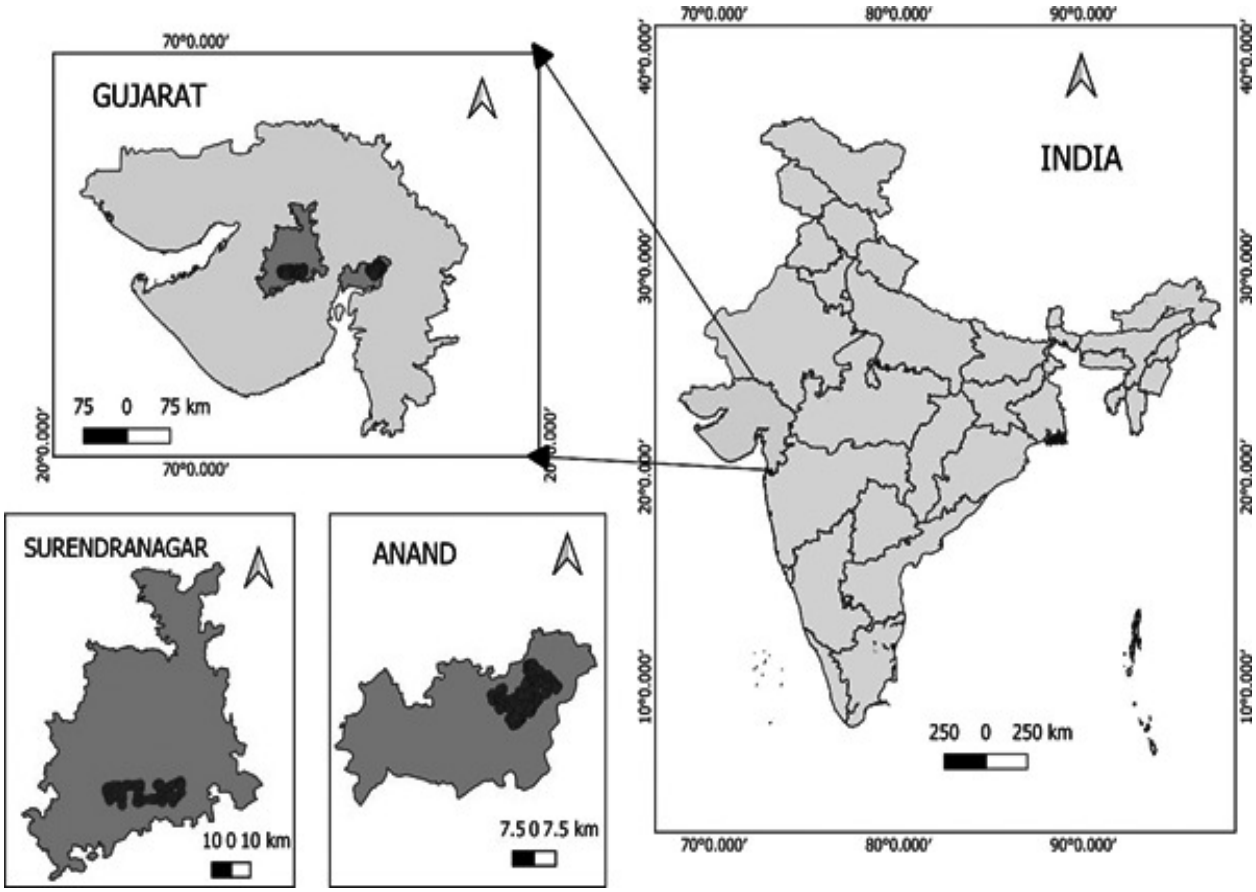

Figure 1. Map showing locations of soil samples collected from Anand and Surendranagar districts

ISRIC World Soil Information System (WoSIS) data

Global SOC data were sourced from the ISRIC World Soil Information System (WoSIS) snapshots (Figure 2). SOC values (g kg^{-1}) were converted to percentage using a factor of 10. From 64,118 profiles, filtering for 0–15 cm depth, Walkley–Black method, and SOC ≤ 10% yielded 18,818 usable points.

Environmental Covariates

Environmental covariates were selected following the SCORPAN framework and included soil, climate, vegetation, and relief variables (Table 2). Spatial resolutions ranged from 1 km (climate) to 30 m (relief). A total of 43 covariates were used for modelling.

Table 2. Environmental covariates used to predict soil organic carbon

Covariate	Source	Spatial Resolution
Soil	Soil Grids 250M v2.0, USDA Soil Taxcnomy	250 m
Climate	World Clim version 1	1 km
Organism	MODIS	250 m
Relief	NASA SRTM	30 m

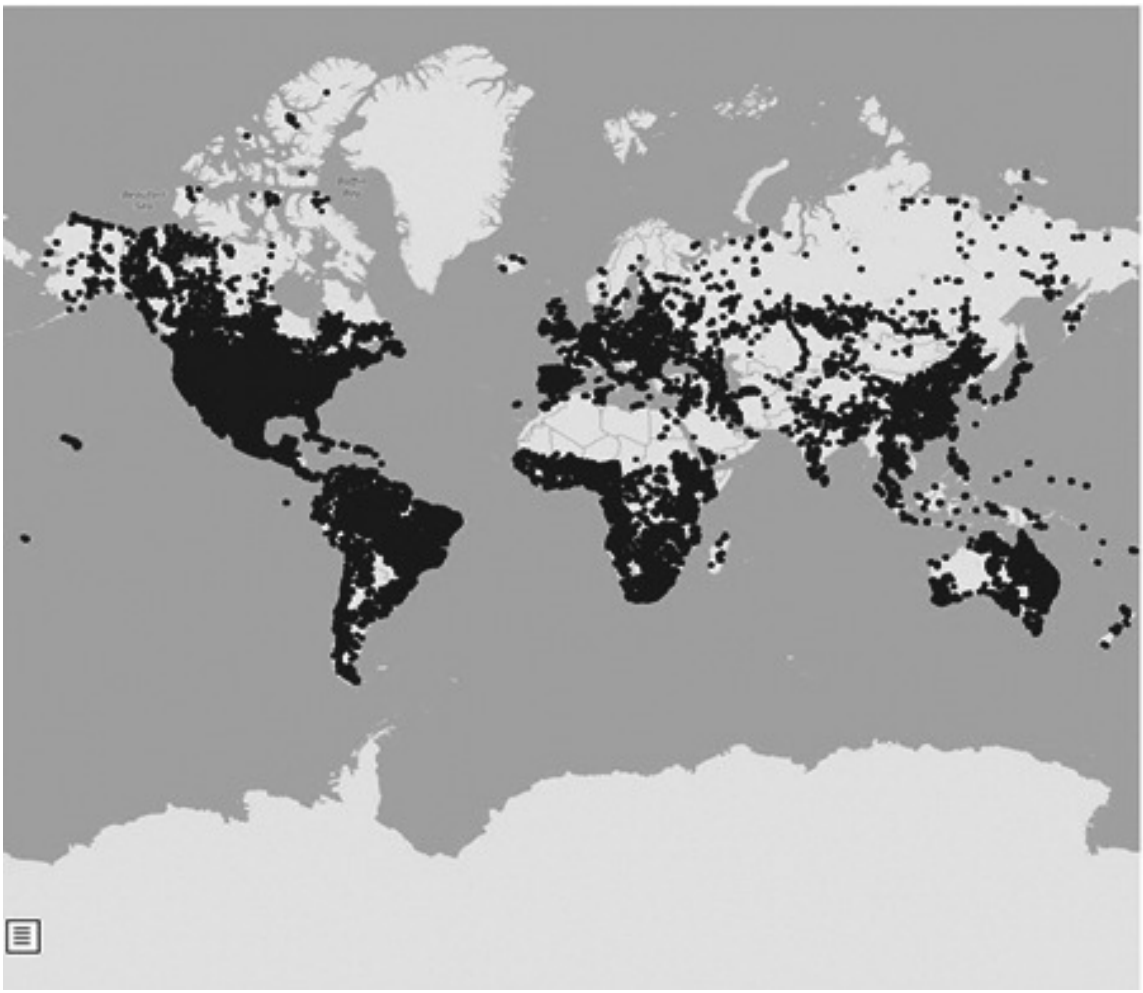

Figure 2. Location of soil profiles provided with WoSIS.
(Source: https://data.isric.org)

Soil Properties

Six soil properties at 0–5 cm depth (Bulk density, CEC, clay, sand, silt, pH) were obtained from SoilGrids 250 m v2.0 via Google Earth Engine (GEE). Descriptions and unit conversions are shown in Table 3.

Climatic Variables

Climate variables (temperature, precipitation, and BIOCLIM variables) were obtained from WorldClim v1 through GEE. All layers were stacked and extracted for local and global datasets (Table 4). Climatic variables originally available at 1-km resolution (WorldClim v1) were resampled to 30 m in Google Earth Engine using its image pyramid framework, which selects the closest lower-resolution pyramid level and applies nearest-neighbour resampling by default. Downscaling coarse-resolution climate layers does not generate new climatic information at finer spatial scales and may introduce smoothing or resampling artefacts. Consequently, the resampled climate variables represent regional-scale climatic gradients rather than true microclimatic variability, and their influence on SOC prediction is interpreted accordingly.

Table 3. Soil properties used in the study

Soil Property	Description	Mapped units	Conversion factor	Conventional units
BD	Bulk density of the fine earth fraction	eg/cm^3	100	kg/dm^3
CEC	Cation Exchange Capacity of the soil	mmol(c)/kg	10	cmol(c)/kg
Clay	Proportion of clayparticles in the fine earth fraction	(< g/kg 0.002 mm)	10	g/100 (%)
Sand	Proportion of sand particles in the fine earth fraction	(> g/kg 0.05 mm)	10	g/100g (%)
Silt	Proportion of silt particles 0.002 mm and ≤ 0.05 mm) in the fine earth fraction	(≥ g/kg	10	g/100g (%)
pH	Soil pH	pHx10	10	pH

Vegetation Attributes

Vegetation indices (EVI and NDVI) were derived from MOD13Q1 (250 m, 16-day composites; 2001–2022). Long-term annual maximum/minimum EVI and NDVI ranges were computed and extracted using GEE.

Table 4. Climatic variables used in the study

Name	Description
tavg	Mean temperature, ^{0}C
tmin	Minimum temperature, ^{0}C
tmax	Maximum temperature, ^{0}C
prec	Precipitation, mm
bio01	Annual mean temperature, ^{0}C
bio02	Mean diurnal range (mean of monthly (max tem - min tem)), ^{0}C
bio03	Isothermality (bio02/bio07 * 100), %
bio04	Temperature seasonality (Standard deviation * 100), ^{0}C
bio05	Max temperature of warnest month, ^{0}C
bio06	Min temperature of coldest month, ^{0}C
bio07	Temperature annual range, ^{0}C
bio08	Mean temperature of wettest quarter, ^{0}C
bio09	Mean temperature of driest quarter, ^{0}C
bio10	Mean temperature of warmest quarter, ^{0}C
bio11	Mean temperature of coldest quarter, ^{0}C
bio12	Annual precipitation, mm
bio13	Precipitation of wettest month, mm
bio14	Precipitation of driest month, mm
bio15	Precipitation seasonality (Coefficient of Variation)
bio16	Precipitation of wettest quarter, mm
bio17	Precipitation of driest quarter, mm
bio18	Precipitation of warmest quarter, mm
bio19	Precipitation of warmest quarter, mm

Topographic Parameters

Topographic variables (Slope, Aspect, Hillshade, Relief, TPI, TRI) were derived from the 30-m SRTM DEM on GEE and extracted for all sample points.

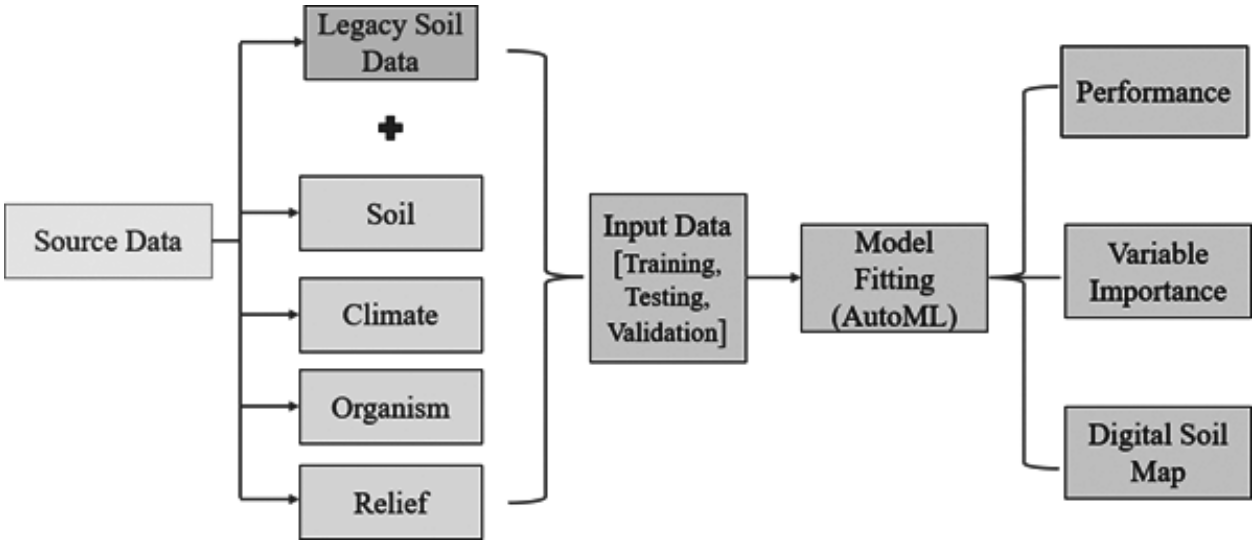

Figure 3. Methodology Flowchart

Data Preparation for SOC Prediction

All covariates were merged into a unified CSV dataset. Environmental rasters were downscaled to 30 m using GEE image pyramids to ensure consistency across layers. Individual rasters were stacked to form a single multiband layer used for prediction modeling. The overall workflow is shown in Figure 3.

Soil Organic Carbon Prediction

Predictive modelling was conducted in RStudio using AutoML with automated hyperparameter optimization; no manual tuning was performed. The response variable was SOC for the local dataset and log-transformed SOC for the global dataset. Log transformation was applied only to the global SOC dataset to address skewness and heteroscedasticity associated with its wider value range, whereas the local dataset exhibited a narrower distribution and did not require transformation. Data were split into training (60%), validation (20%), and testing (20%). AutoML (300-second runtime) automatically evaluated multiple algorithms (GBM, DRF/XRT, GLM, Deep Learning, and Stacked Ensemble) with cross-validation (Table 5). Upon completion, the leaderboard was examined to identify the top-performing models based on evaluation metrics such as Root Mean Squared Error (RMSE) and R^2.

Permutation Variable Importance

Variable importance was assessed using permutation importance through the

H_2O interface. The Fisher–Yates shuffle was applied to each predictor, and loss in model accuracy (difference in RMSE or R^2 from baseline) quantified its importance. This method provided insights into the relative influence of climate, soil, vegetation, and relief factors on SOC prediction.

Table 5. Models used in AutoML

Model	Description
DRF	This includes both the Distributed Random Forest (DRF) and Extremely Randomized Trees (XRT) models.
GLM	Generalized Linear Model with regularization
GBM	Gradient Boosting Machine
Deep Learning	Fully-connected multi-layer artificial neural network.
Stacked Ensemble	Stacked Ensembles, includes an ensemble of all the base models and ensembles using subsets of the base models.

Results and Discussion

Prediction Model Performance

Local Scale model using ground truth data

The Gradient Boosting Machine (GBM) stood out as the best model among the algorithms tested for predicting SOC content at the local scale. It achieved a R^2 value of 0.49 on the training data and 0.35 on the testing data and RMSE values of 0.05 and 0.06 on the training and testing data, respectively, indicating its ability to capture the relationship between environmental factors and SOC. algorithms tested for predicting SOC content at the local scale. It achieved a R^2 value of 0.49 on the training data and 0.35 on the testing data and RMSE values of 0.05 and 0.06 on the training and testing data, respectively, indicating its ability to capture the relationship between environmental factors and SOC. The observed versus predicted plots for both training and testing data revealed a strong linear trend between observed and predicted SOC values, indicating that the model captured the dominant relationships between SOC and the selected environmental covariates (Figure 4).

Global Scale model using WoSIS data

For the global-scale model using WoSIS data, the Stacked Ensemble algorithm emerged as the top-performing model. With high R^2 values of 0.87 on the training set and 0.70 on the testing set, and RMSE values of 0.29 and 0.33 on the training and testing data, respectively, the Stacked Ensemble algorithm exhibited strong predictive performance in estimating SOC content. Examination of the observed versus predicted plots further confirmed the model's effectiveness, revealing its ability to capture the underlying patterns

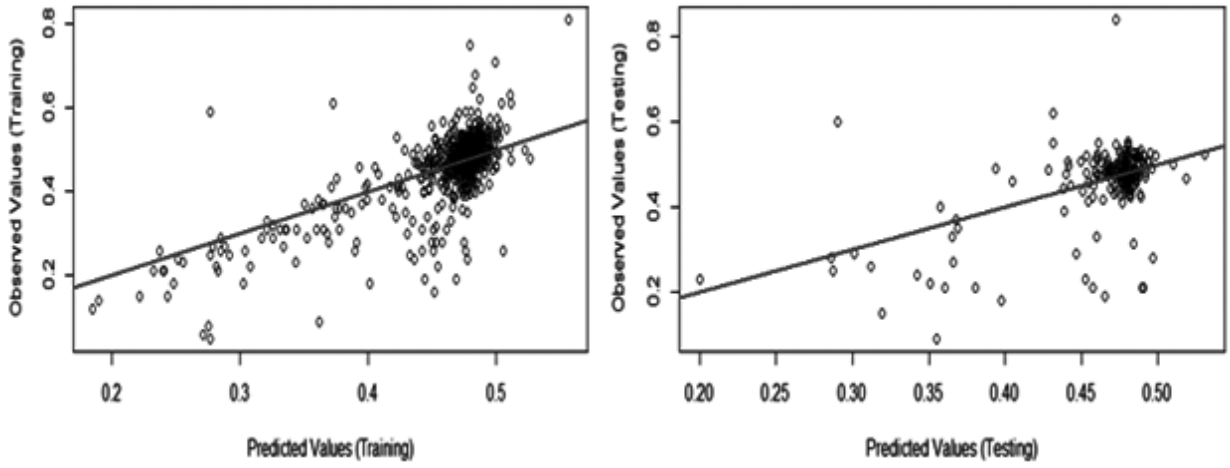

Figure 4. a) observed vs. predicted for training data and b) observed vs. predicted for testing data in the local scale model

and relationships between the environmental covariates and SOC content. Observed versus predicted plots showed a strong linear trend between observed and predicted SOC values, confirming the ability of the Stacked Ensemble model to represent underlying SOC–environment relationships (Figure 5). Therefore, it can be concluded that the Stacked Ensemble model provides a reliable tool for predicting SOC content at the global scale, offering valuable insights into soil dynamics and environmental processes, capturing better variability than the local model (Table 6). The digital maps of SOC (%) produced by local and global models are shown in (Figure 6).

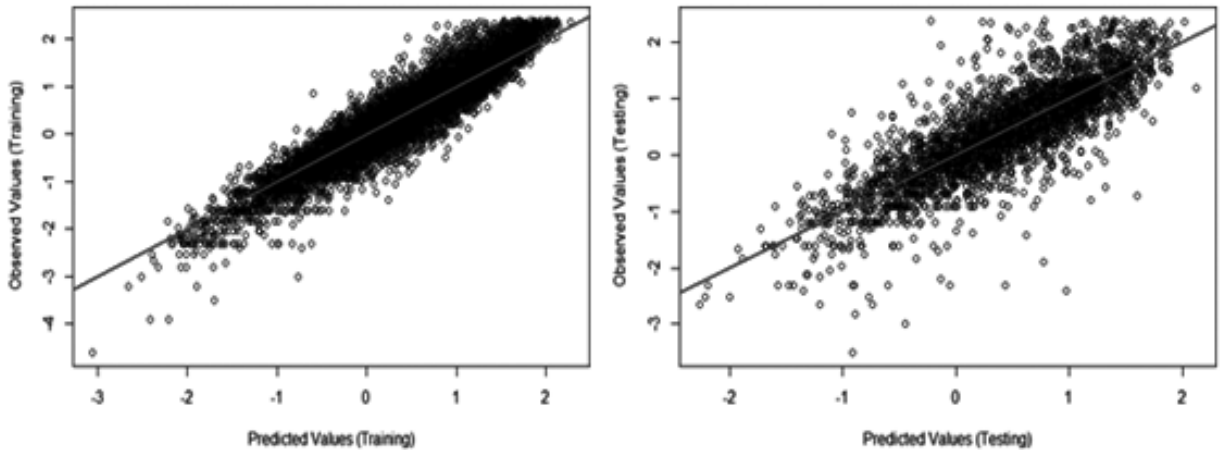

Figure 5. a) observed V/S predicted for training data and b) observed vs. predicted for testing data in the global scale model

Table 6. Performance matrix of local and global models

	Local model		Global model	
	Training	**Testing**	**Training**	**Testing**
R^2	0.49	0.35	0.87	0.70
RMSE	0.05	0.06	0.29	0.33

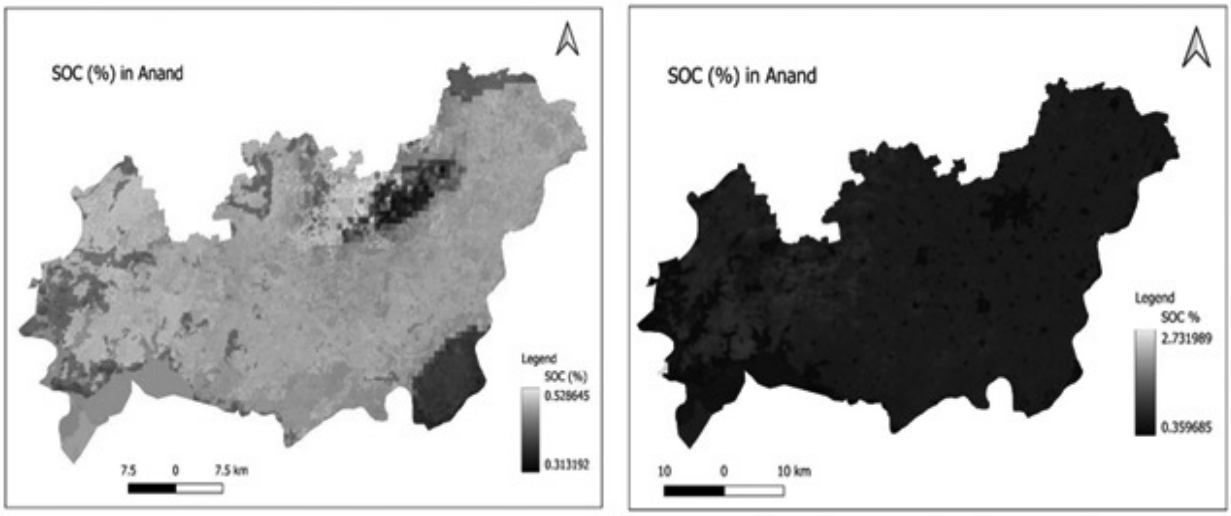

Figure 6.a) SOC (%) map for Anand using the local model and b) SOC (%) map for Anand using the global model

Variable Importance

Variable Importance for the local scale model

In the variable importance analysis for the local-scale model, it was found that bio12 (Annual precipitation, mm) emerged as the most influential variable, followed by elevation and bio04 (Temperature seasonality (Standard deviation * 100), ° C). Among the top 10 important variables, there were four from Climate, four from Soil and two from Relief, indicating a diverse range of factors impacting SOC content prediction (Figure 7). Notably, in the Gujarat region, bio12 appeared as the most influential variable, indicating that variations in this climatic variable would exert the most

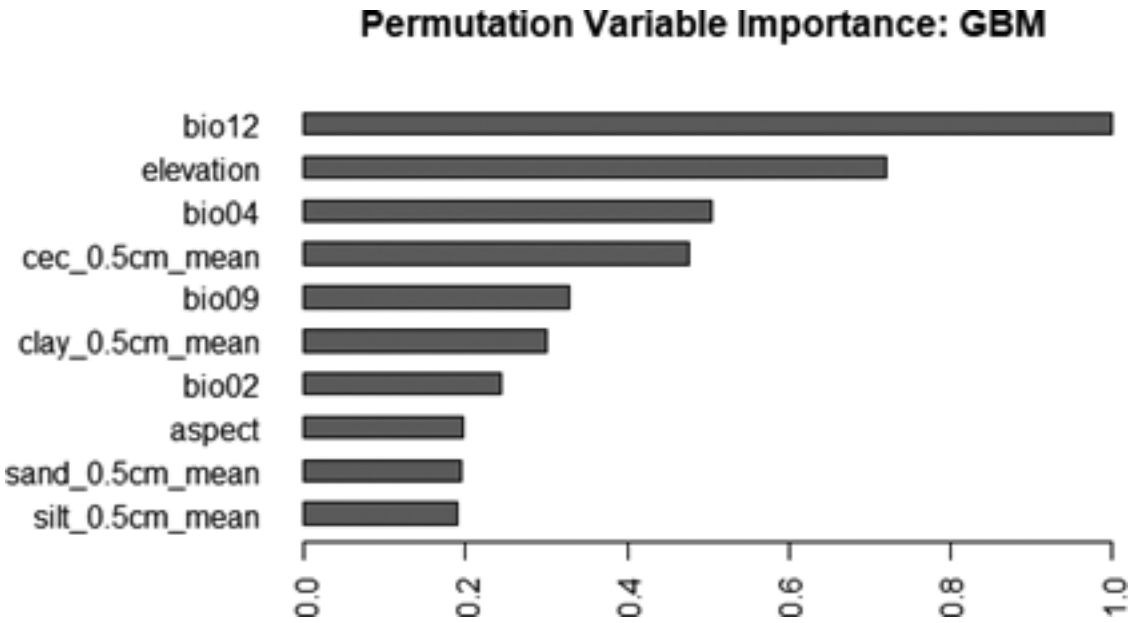

Figure 7. Permutation variable importance for the local scale model

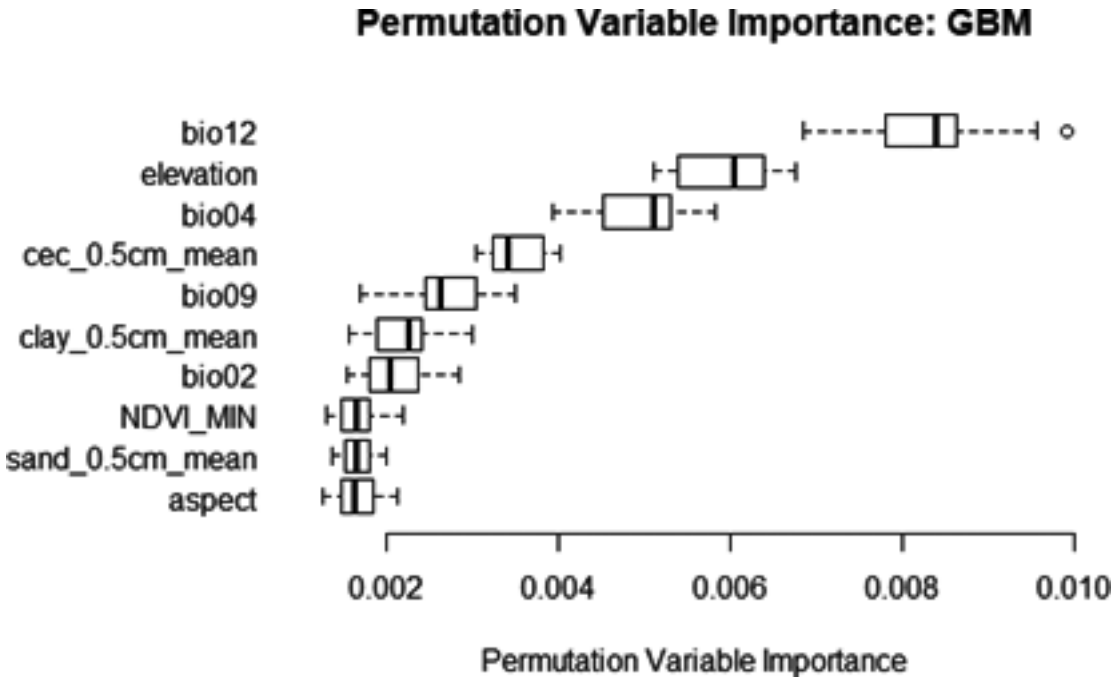

Figure 8. Permutation variable importance Boxplots for the local scale model

significant influence on SOC content prediction (Figure 8). This underscores the importance of considering regional climatic conditions, such as mean temperature during the driest quarter and precipitation, when assessing SOC dynamics and developing predictive models at the local scale.

Variable Importance for the global scale model

In the variable importance analysis for the global-scale model, long-term average annual max EVI (NDVI_MAX) emerged as the most influential variable, as determined by Permutation Variable Importance. Among the top 10 important variables, three were Soil properties, three were Climatic variables, three were Vegetation parameters, and one was a Relief parameter (Figure 9). This diversity in influential variables underscores the complex interplay of environmental factors influencing SOC content prediction at a global scale. Additionally, analysis of boxplots revealed that Vegetation and Climatic variables exerted the most prominent effects on the prediction of SOC content, further highlighting their significance in driving SOC dynamics on a broader spatial scale (Figure 10). These findings underscore the importance of considering multiple environmental variables, particularly those related to vegetation and climate, when assessing SOC dynamics and developing predictive models at the global scale.

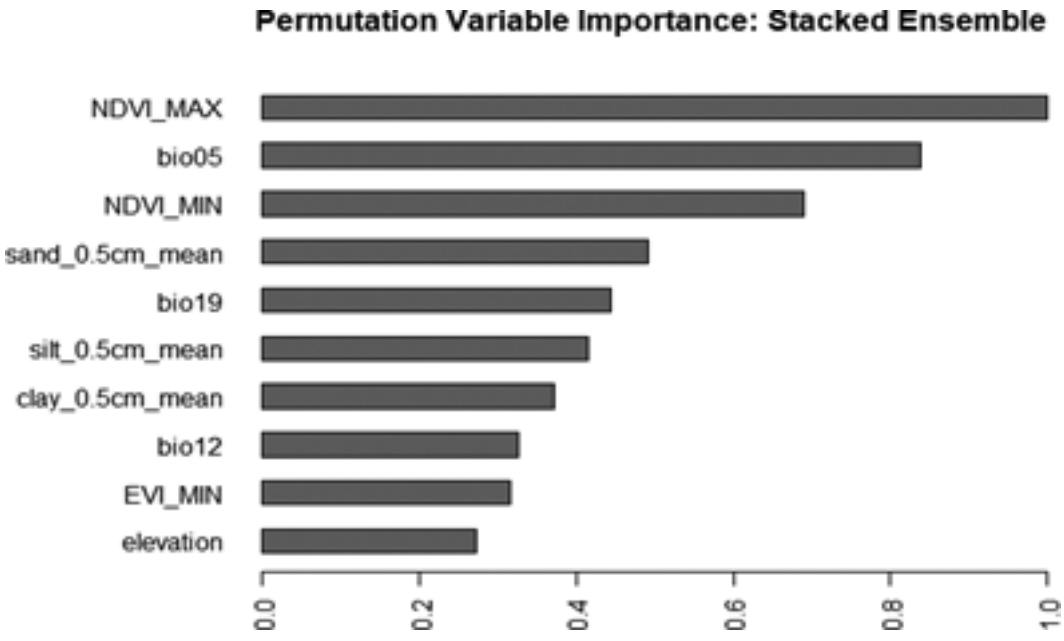

Figure 9. Permutation variable importance for the global scale model

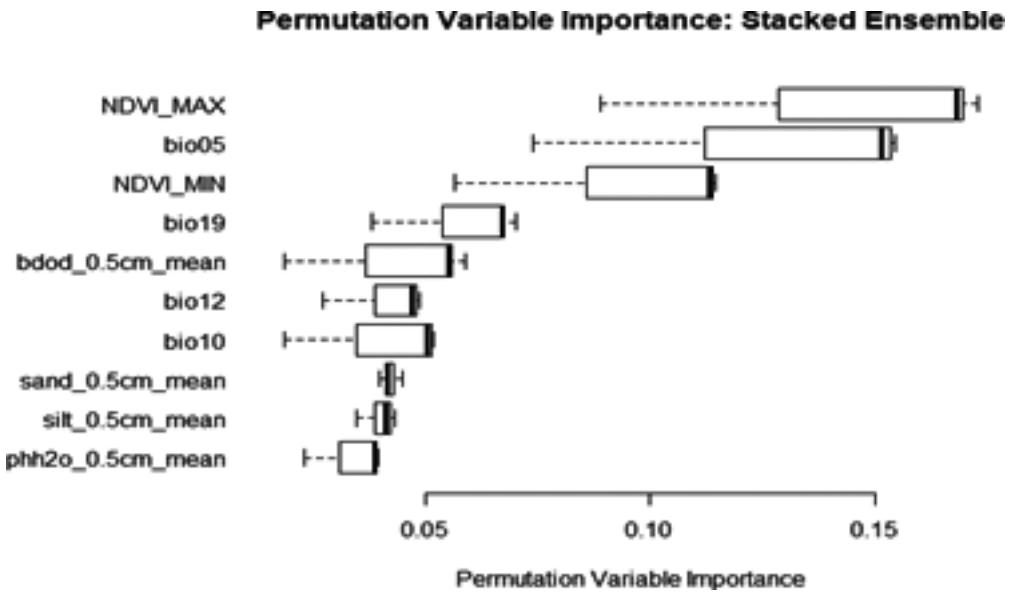

Figure 10. Permutation variable importance boxplot for global scale model

Conclusion

This study demonstrates that Automatic Machine Learning can effectively integrate multiscale remote sensing, climatic, soil, and terrain data to generate high-resolution maps of SOC. The Gradient Boosting Machine performed best at the local scale, while the Stacked Ensemble model showed superior performance at the global scale, highlighting the importance of scale-aware model selection. Variable-importance analysis consistently identified annual precipitation and long-term maximum EVI as dominant predictors of SOC, emphasizing the combined role of climate and vegetation dynamics in regulating SOC variability. From a practical perspective, the generated SOC maps can support site-specific soil and nutrient management, identification of low-carbon zones requiring restorative practices, and land-use planning under climate variability. For policymakers, these spatial products can aid in carbon accounting, prioritization of soil conservation interventions, and monitoring of soil health indicators at regional scales, particularly in data-scarce environments. Several limitations should be acknowledged. Climatic variables were downscaled from coarse-resolution datasets and therefore represent regional climatic gradients rather than true microclimatic variability. In addition, differences in sampling density and SOC value distributions between local and global datasets influenced model performance and comparability. While ensemble models demonstrated strong predictive skill, their complexity also limits direct physical interpretability. Future research should focus on incorporating higher-resolution hyperspectral imagery, proximal sensing data, and deep learning architectures to better capture soil–vegetation–climate interactions at finer scales. Expanding the framework to

include temporal dynamics, uncertainty quantification, and independent regional validations would further enhance the robustness and applicability of SOC mapping for sustainable land management and climate-resilient agriculture.

References

Adhikari, P., Sen, D. and Uphoff, N. 2010. System of rice intensification as a resource-conserving methodology: Contributing to food security in an era of climate change. *SATSA Mukhapatra-Annual Technical Issue* **14**: 26–42.

Akpa, S. I., Odeh, I. O., Bishop, T. F. and Hartemink, A. E. 2014. Digital mapping of soil particle-size fractions for Nigeria. *Soil Science Society of America Journal* **78** (6): 1953–1966.

Arrouays, D., Grundy, M. G., Hartemink, A. E., Hempel, J. W., Heuvelink, G. B., Hong, S. Y. and Zhang, G. L. 2014. GlobalSoilMap: Toward a fine-resolution global grid of soil properties. *Advances in Agronomy* **125**: 93–134.

Batjes, N. H. 1996. Total carbon and nitrogen in the soils of the world. *European Journal of Soil Science* **47**(2): 151–163.

Batjes, N. H. and Sombroek, W. G. 1997. Possibilities for carbon sequestration in tropical and subtropical soils. *Global Change Biology* **3**(2): 161–173.

Brady, N. C. and Weil, R. R. 2008. *The Nature and Properties of Soils*. 13th ed. Prentice Hall, Upper Saddle River, NJ. pp. 662–710.

Breiman, L., Friedman, J. H., Olshen, R. A. and Stone, C. J. 1984. *Classification and Regression Trees*. Wadsworth Statistics/Probability Series, Wadsworth & Brooks.

Conant, R. T., Ogle, S. M., Paul, E. A. and Paustian, K. 2011. Measuring and monitoring soil organic carbon stocks in agricultural lands for climate mitigation. *Frontiers in Ecology and Environment* **9**(3): 169–173.

Cressie, N. and Johannesson, G. 2008. Fixed rank kriging for very large spatial data sets. *Journal of the Royal Statistical Society: Series B (Statistical Methodology)* **70**(1): 209–226.

Denton, F., Wilbanks, T. J., Abeysinghe, A. C., Burton, I., Gao, Q., Lemos, M. C. and Warner, K. 2014. Climate-resilient pathways: Adaptation, mitigation, and sustainable development. *Climate Change*. pp. 1101–1131.

Dobermann, A. and Ping, J. L. 2004. Geostatistical integration of yield monitor data and remote sensing improves yield maps. *Agronomy Journal* **96**(1): 285–297.

Foody, G. M. 2002. Status of land cover classification accuracy assessment. *Remote Sensing of Environment* **80**(1): 185–201.

Friedl, M. A. and Brodley, C. E. 1997. Decision tree classification of land cover from remotely sensed data. *Remote Sensing of Environment* **61**(3): 399–409.

Giasson, E., Clarke, R. T., Inda Júnior, A. V., Merten, G. H. and Tornquist, C. G. 2006. Digital soil mapping using logistic regression on terrain parameters in Southern Brazil. *Scientia Agricola* **63**: 262–268.

GSP. 2017. *Global Soil Organic Carbon Map – Leaflet*. FAO, Rome, Italy.

Henderson, B. L., Bui, E. N., Moran, C. J. and Simon, D. A. P. 2005. Australia-wide predictions of soil properties using decision trees. *Geoderma* **124**(3–4): 383–398.

Hengl, T., Heuvelink, G. B. and Stein, A. 2004. A generic framework for spatial prediction of soil variables based on regression-kriging. *Geoderma* **120**(1–2): 75–93.

Heuvelink, G. B. M. and Webster, R. 2001. Modelling soil variation: Past, present, and future. *Geoderma* **100**(3–4): 269–301.

Huang, J., Nhan, T., Wong, V. N., Johnston, S. G., Lark, R. M. and Triantafilis, J. 2014. Digital soil mapping of a coastal acid sulfate soil landscape. *Soil Research* **52**(4): 327–339.

Jenny, H. 1941. *Factors of Soil Formation – A System of Quantitative Pedology*. McGraw Hill, New York, NY.

Kempen, B., Brus, D. J., Heuvelink, G. B. M. and Stoorvogel, J. J. 2009. Updating the 1:50,000 Dutch soil map using legacy soil data: A multinomial logistic regression approach. *Geoderma* **151**: 311–326.

Kovaèevic, M., Bajat, B. and Gajiæ, B. 2010. Soil type classification and estimation of soil properties using support vector machines. *Geoderma* **154**: 340–347.

Lagacherie, P. and McBratney, A. B. 2006. Spatial soil information systems and spatial soil inference systems: Perspectives for digital soil mapping. *Developments in Soil Science* **31**: 3–22.

Lal, R. 1998. Soil erosion impact on agronomic productivity and environment quality. *Critical Reviews in Plant Sciences* **17**(4): 319–464.

Lal, R. 2004. Soil carbon sequestration impacts on global climate change and food security. *Science* **304** (5677): 1623–1627.

Malone, B. P., McBratney, A. B., Minasny, B. and Laslett, G. M. 2009. Mapping continuous depth functions of soil carbon storage and available water capacity. *Geoderma* **154**(1–2): 138–152.

Mansuy, N., Thiffault, E., Paré, D., Bernier, P., Guindon, L., Villemaire, P., Poirier, V. and Beaudoin, A. 2014. Digital mapping of soil properties in Canadian managed forests at 250 m resolution using the k-nearest neighbor method. *Geoderma* **235–236**: 59–73.

Martin, P. D., Malley, D. F., Manning, G. and Fuller, L. 2002. Determination of soil organic carbon and nitrogen at the field level using near-infrared spectroscopy. *Canadian Journal of Soil Science* **82**: 413–422.

McBratney, A. B., Odeh, I. O., Bishop, T. F., Dunbar, M. S. and Shatar, T. M. 2000. An overview of pedometric techniques for use in soil survey. *Geoderma* **97** (3–4): 293–327.

McBratney, A. B., Santos, M. M. and Minasny, B. 2003. On digital soil mapping. *Geoderma* **117**(1–2): 3–52.

McCarty, G. W. and Reeves III, J. B. 2001. Development of rapid instrumental methods for measuring soil organic carbon. In: Lal, R. (Ed.), *Assessment*

Methods for Soil Carbon. Lewis Publishers, Boca Raton. pp. 371–380.

McKenzie, N. J. and Ryan, P. J. 1999. Spatial prediction of soil properties using environmental correlation. *Geoderma* **89**(1–2): 67–94.

Minasny, B. and McBratney, A. B. 2016. Digital soil mapping: A brief history and some lessons. *Geoderma* **264**: 301–311.

Minasny, B., McBratney, A. B., Malone, B. P. and Wheeler, I. 2013. Digital mapping of soil carbon. In: Sparks, D. L. (Ed.), *Advances in Agronomy*. Academic Press. pp. 1–47.

Nijbroek, R., Piikki, K., Söderström, M., Kempen, B., Turner, K. G., Hengari, S. and Mutua, J. 2018. Soil organic carbon baselines for land degradation neutrality: Map accuracy and cost tradeoffs with respect to complexity in Otjozondjupa, Namibia. *Sustainability* **10**(5): 1610.

Oliver, M. A. 1987. Geostatistics and its application to soil science. *Soil Use and Management* **3**(1): 8–20.

Odeh, I. O. and McBratney, A. B. 2000. Using AVHRR images for spatial prediction of clay content in the lower Namoi Valley of eastern Australia. *Geoderma* **97**(3–4): 237–254.

Powers, J. S. and Schlesinger, W. H. 2002. Relationships among soil carbon distributions and biophysical factors at nested spatial scales in rain forests of northeastern Costa Rica. *Geoderma* **109**(3–4): 165–190.

Rossel, R. A. V. and Bouma, J. 2016. Soil sensing: A new paradigm for agriculture. *Agricultural Systems* **148**: 71–74.

Salter, P. J. and Haworth, F. 1961. The available-water capacity of a sandy loam soil: I. A critical comparison of methods of determining soil moisture content at field capacity and permanent wilting percentage. *Journal of Soil Science* **12**(2): 326–334.

Sanchez, P. A., Ahamed, S., Carré, F., Hartemink, A. E., Hempel, J., Huising, J. and Zhang, G. L. 2009. Digital soil map of the world. *Science* **325**(5941): 680–681.

Schoonover, J. E. and Crim, J. F. 2015. An introduction to soil concepts and the role of soils in watershed management. *Journal of Contemporary Water Research and Education* **154**(1): 21–47.

Shibu, M. E., Leffelaar, P. A., Van Keulen, H. and Aggarwal, P. K. 2006. Quantitative description of soil organic matter dynamics—A review of approaches with reference to rice-based cropping systems. *Geoderma* **137**(1–2): 1–18.

Walkley, A. and Black, I. A. 1934. An examination of the Degtjareff method for determining soil organic matter and a proposed modification of the chromic acid titration method. *Soil Science* **37**(1): 29–38.